ACS MEASUREMENT SCIENCE Au
AN OPEN ACCESS JOURNAL OF THE AMERICAN CHEMICAL SOCIETY

pubs.acs.org/measureau
Article

Enhancing Quantitative Analysis of Xenobiotics in Blood Plasma through Cross-Matrix Calibration and Bayesian Hierarchical Modeling

Published as part of ACS Measurement Science Au virtual special issue "2023 Rising Stars".

Nipunika H. Godage, Song S. Qian, Erasmus Cudjoe, and Emanuela Gionfriddo*

Cite This: ACS Meas. Sci. Au 2024, 4, 127−135
Read Online

ACCESS | Metrics & More | Article Recommendations | Supporting Information

ABSTRACT: This study addresses the challenges of matrix effects and interspecies plasma protein binding (PPB) on measurement variability during method validation across diverse plasma types (human, rat, rabbit, and bovine). Accurate measurements of small molecules in plasma samples often require matrix-matched calibration approaches with the use of specific plasma types, which may have limited availability or affordability. To mitigate the costs associated with human plasma measurements, we explore in this work the potential of cross-matrix-matched calibration using Bayesian hierarchical modeling (BHM) to correct for matrix effects associated with PPB. We initially developed a targeted quantitative approach utilizing biocompatible solid-phase microextraction coupled with liquid chromatography−mass spectrometry for xenobiotic analysis in plasma. The method was evaluated for absolute matrix effects across human, bovine, rat, and rabbit plasma comparing pre- and postmatrix extraction standards. Absolute matrix effects from 96 to 108% for most analytes across plasma sources indicate that the biocompatibility of the extraction phase minimizes interference coextraction. However, the extent of PPB in different media can still affect the accuracy of the measurement when the extraction of small molecules is carried out via free concentration, as in the case of microextraction techniques. In fact, while matrix-matched calibration revealed high accuracy, cross-matrix calibration (e.g., using a calibration curve generated from bovine plasma) proved inadequate for precise measurements in human plasma. A BHM was used to calculate correction factors for each analyte within each plasma type, successfully mitigating the measurement bias resulting from diverse calibration curve types used to quantify human plasma samples. This work contributes to the development of cost-effective, efficient calibration strategies for biofluids. Leveraging easily accessible plasma sources, like bovine plasma, for method optimization and validation prior to analyzing costly plasma (e.g., human plasma) holds substantial advantages applicable to biomonitoring and pharmacokinetic studies.

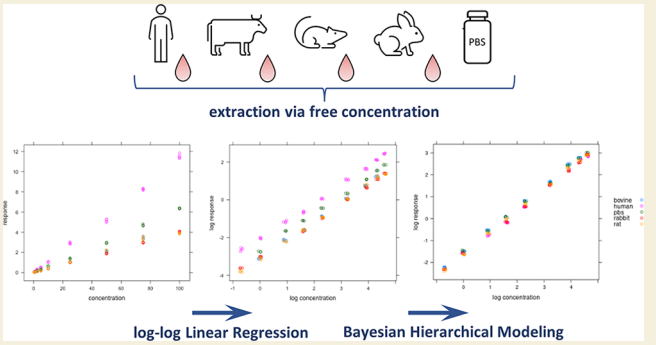

KEYWORDS: *solid-phase microextraction (SPME), xenobiotics, matrix effect (ME), calibration, Bayesian hierarchical modeling*

1. INTRODUCTION

Biomonitoring involves the systematic investigation of organisms' exposure to xenobiotics to identify potential hazards and effects on biological functions.[1] Xenobiotics are chemicals (e.g., pesticides and pharmaceuticals) that are foreign to a living or ecological system and enter these systems through environmental exposure or food consumption.[1] Biomonitoring has several applications related to human and animal health, such as epidemiological investigations, clinical studies, emergency response decision processes, and identification of preclinical indicators.[1] In terms of exposure assessment, biomonitoring involves the study of exposure levels, trends, pathways of emerging chemicals, and results in the identification of susceptible populations.[1] An organism's exposure to xenobiotics can be evaluated by analyzing its biospecimens, such as tissues, blood and its derivatives, saliva, and urine.[2] To accurately and precisely determine the levels of targeted analytes in biological samples, liquid or gas chromatography coupled to tandem mass spectrometry, among others, is commonly used.[3] However, these techniques are not immune to matrix effects.[3]

Received: September 1, 2023
Revised: November 18, 2023
Accepted: November 20, 2023
Published: December 5, 2023

Matrix effects occur due to alteration of the ionization process of target analytes when coeluting compounds are present in the sample matrix which in turn can affect biomonitoring studies by altering the sensitivity, accuracy, and precision of the measurements.[4] Analyte response can reduce or intensify (ion suppression or enhancement, respectively) as a result of matrix effects.[4] Particularly, when employing electrospray ionization (ESI) technique matrix effects can become pronounced when coeluted matrix components affect analytes' signal intensity due to competition for available charges and access to droplet surfaces for gas-phase emission.[4]

The unique composition of biological specimens can generate distinct matrix effects during analysis especially when clean-up and preconcentration of the sample are not effective in minimizing the extent of matrix components coextracted with the targeted analytes. The most commonly used biological matrices for biomonitoring are blood and its derivatives (e.g., plasma, serum) and urine.[5] Phospholipids, which make up the majority of the membrane of cells, are the primary matrix components that cause matrix effects during liquid chromatography−mass spectrometry (LC-MS) analysis of complex biological fluids.[6] In addition, blood plasma contains proteins—albumin, globulins, and fibrinogen—while urine contains salts (potassium, sodium), creatinine, and urea that can contribute to the matrix effect during analysis.[7]

Matrix effects can also vary among a given biofluid across animal species, due to differences in the type of components and their concentrations, which in turn can cause biased results during biomonitoring studies and during preclinical bioanalytical measurements, used to predict the preclinical parameters in human plasma.[8,9] Even within a single species, variations in matrix component composition, such as lipid content in plasma, can arise due to factors like diet and metabolic activity, potentially affecting the extent of matrix effects.[8] In light of the above, it is important to carefully assess the occurrence of matrix effects for each species during quantitative analysis in order to verify that quantification bias for matrix effects remains within the limits defined by regulatory guidelines.[8,10,11] Although matrix effects during LC-MS analysis cannot be completely avoided, they can be minimized or compensated for by optimizing sample preparation procedures. In terms of bioanalysis, conventional sample preparation methods such as liquid−liquid extraction, protein precipitation, and solid-phase extraction were commonly applied to achieve cleaner extract to avoid matrix components interfering with the analysis.[12−14]

In this context, solid-phase microextraction (SPME) techniques provide remarkable advantages over conventional sample preparation methods due to the biocompatibility of the extraction phases. Matrix compatibility of the SPME extraction phase is an essential requirement to mitigate matrix effects caused by complex biological matrices. Matrix-compatible SPME extraction phases are resistant to biofouling, permitting direct contact with complex samples while selectively extracting analytes.[15]

Even though the use of matrix-compatible SPME in sample preparation of biofluids has proven the ability to reduce absolute matrix effects, it is crucial to consider the effect of plasma protein binding (PPB) on the extraction recoveries, considering that SPME only extract analytes via free concentration. This is a type of matrix effect often neglected in the literature, and this work, for the first time in the best authors' knowledge, addresses this knowledge gap.

An array of physicochemically different pharmaceuticals and pesticides were selected in this study to assess the matrix effect related to mammalian plasma from different species (rat, rabbit, bovine, human). Calibration curves conducted in PBS, bovine, rat, or rabbit plasma, which are considered more affordable to obtain, were tested to correct the responses obtained by extraction from human plasma samples. To cross-calculate the accuracy of human plasma samples, we used plasma calibration curves from different species (rat, rabbit, and bovine) and investigated correction factors using Bayesian hierarchical modeling (BHM) to combine calibration curves from multiple matrices. This research aims to develop a cost-effective biomonitoring method with a convenient approach to correct for instrumental and PPB-related matrix effects.

2. EXPERIMENTAL CONDITIONS AND METHODS

2.1. Materials and Instrumentation

The reference standards of diazepam, lorazepam, alprazolam, methaqualone, omeprazole, acetochlor, atrazine, metolachlor, cyprodinil, and chlorpyrifos-methyl were purchased from Sigma-Aldrich (St. Louis, MO, USA). The physicochemical properties of the analytes and the rationale behind the selection of the targeted analytes are listed in Table S1. Diazepam-D_5, obtained from Cerilliant-Sigma-Aldrich (Austin, MO, USA), and Metolachlor-D_6, purchased from Toronto Research Chemicals (North York, Ontario, Canada), were used as deuterated internal standards. Pooled bovine plasma, rabbit plasma, rat plasma, and human plasma preserved in sodium citrate were purchased from Innovative Research (MI, USA). The authors are not aware of any ethical issue associated with plasma collection; Innovative research is ISO, Food and Drug Administration (FDA), USDA, and EPA approved. C_{18}/PAN SPME fibers were provided by Millipore Sigma (Bellefonte, PA, USA). The thickness and coating length of the fiber were 45 μm and 1.5 cm, respectively. LC-MS grade methanol, water, ammonium formate, and formic acid were obtained from Fisher Scientific (Waltham, MA, USA), and phosphate-buffered saline (PBS) was purchased from Sigma-Aldrich (St. Louis, MO, USA).

2.2. Instrumentation and Data Processing

Analysis of the drugs and pesticides was performed using a PerkinElmer QSight LX50 UHPLC, autosampler, and column compartment (PerkinElmer Inc., Waltham, MA, USA) coupled to a triple quadrupole mass spectrometer PerkinElmer QSight 220 (PerkinElmer Inc. Waltham, MA, USA). The mass spectrometer was operated in positive ESI mode. The data acquisition was set to the multiple reaction monitoring (MRM) mode. The optimized MRM transitions and operational conditions of the mass spectrometer are summarized in Tables S2 and S3. Nitrogen gas flow for the ESI source, the laminar flow ion guide, and the collision cell was provided by using a Parker/Balston nitrogen generator system (Parker Hannifin Corporation, Lancaster, NY, USA). Separation of the analytes was achieved by using a 100 mm × 4.6 mm × 2.7 μm Raptor C_{18} column (Restek Corporation, Bellefonte, PA, USA), at a flow rate of 0.7 mL min^{-1} and a column temperature of 30 °C. The optimized chromatographic conditions are listed in Table S4. The chromatographic run was 7 min. The gradient was applied with 0.1% (v/v) formic acid and 5 mM ammonium formate in MeOH:water (5:95, v/v) as mobile phase A and 0.1% (v/v) formic acid and 5 mM ammonium formate in MeOH:water (95:5, v/v) as mobile phase B. Data acquisition and processing were performed with Simplicity 3Q software (version 1.8.2006.12348) (PerkinElmer Inc., Waltham, MA USA). Further statistical studies were performed using Excel 365 (Microsoft Corp., Albuquerque, NM, USA). The most abundant mass transition for each analyte was selected as a quantifier, and the second most abundant transition was monitored as a qualifier. The mass (ng)

https://doi.org/10.1021/acsmeasuresciau.3c00049
ACS Meas. Sci. Au 2024, 4, 127−135

extracted by the SPME fibers was calculated by calibrating the instrument using standard analyte solutions at known concentrations. SPME calibration curves were prepared by plotting the peak area ratios of the analyte and IS against their concentration ratios. The BHM computation code was written and executed by using R (version 4.1.1). Correction factors for cross-matrix calibration were calculated in Excel 365 (Microsoft Corp., Albuquerque, NM, USA).

2.3. Standards Preparation

Pharmaceutical and pesticide standards were prepared in LC-MS grade methanol. All the analytical standards were at a concentration of 1 mg mL^{-1}. Deuterated standards (Diazepam-D_5, Metolachlor- D_6) were at the concentration of 0.1 mg mL^{-1}. To ensure adequate analyte sensitivity for the method optimization, two separate mixtures were prepared to contain drugs and pesticides in concentrations ranging from 5 to 12 mg L^{-1}. All the working solutions were prepared in methanol and stored at −20 °C until use.

2.4. Sample Preparation and Method Optimization

SPME method optimization was conducted in bovine plasma. Ten milliliters of bovine plasma was spiked with 50 μL of drug and pesticide working solutions separately to achieve the final concentration of analytes at 25−60 μg L^{-1}. The organic solvent content in the plasma during analyte spiking was maintained at 1%, to avoid disturbing the partition of the analytes between the sample and the extraction phase.

2.5. Sample Preparation for SPME Calibration Levels and Quality Control (QC) Samples

Matrix-matched SPME calibrations were conducted in PBS and rat, rabbit, bovine, and human plasma. To spike the calibration curve levels, a series of spiking mixtures at 2.5, 6.25, 12.5, 25, 125, 250 μg L^{-1} and 1.25, 2.5, 12.5, 25 mg L^{-1} were prepared. Spiking mixtures at 8.75, 62.5 μg L^{-1} and 0.625, 6.25, and 18.75 mg L^{-1} were prepared to spike the QC samples. A spiking mixture containing the deuterated internal standards was prepared at a concentration of 5 mg L^{-1}. All the spiking mixtures were prepared in methanol and stored at −20 °C until use. Plasma aliquots of 2 mL were spiked with 8 μL of each spiking solution. All the spiked plasma samples were vortexed for 1 min and incubated overnight at 4 °C to allow binding equilibria between analytes and the plasma to take place. The plasma was allowed to equilibrate at room temperature prior to extraction and divided into three aliquots of 430 μL to obtain three replicates of each calibration point.

2.6. SPME Fiber Extraction Procedure

The targeted analytes were extracted from plasma samples by using C_{18}/PAN fibers. Fibers were first preconditioned in 1:1 (v:v) MeOH:water for 10 min and then rinsed with ultrapure water for 10 min to remove any organic solvent residue remaining in the fiber extraction phase prior to the extraction process. During the extraction, fiber extraction phase was directly immersed in the sample for 45 min at 1500 rpm at room temperature (20 °C ± 2 °C). After extraction, fibers were rinsed with ultrapure water for 10 s to remove any loosely bound matrix component from the surface of the fiber extraction phase. Then, fiber desorption was conducted at 1500 rpm for 45 min in a vial with an insert filled with 320 μL of desorption solvent at the volume ratio of 2:2:1 of ACN:MeOH:water. Immediately after desorption, extracts were stored at −20 °C until analysis.

2.7. Calibration Strategy and Method Validation

The method validation was conducted in accordance with the FDA guidelines for biological sample analysis in terms of stability, selectivity, a lower limit of quantitation (LLOQ), linearity, accuracy, and precision. Matrix-matched calibration with internal standard correction was used as the calibration strategy. Each calibration in plasma samples from different species (bovine, rat, rabbit, human) and PBS included 10 calibration levels ranging from 0.01 to 100 μg L^{-1}. The linear regression of the calibration curves was established using the weighted least-squares method with a weighting factor of $1/X$. QC samples were evaluated to calculate the accuracy and precision at intermediate concentrations of 0.035, 2.5, 25, and 75 μg L^{-1} within the linear dynamic range of all of the targeted analytes. The bias of the accuracy and precision should be within ±15% and <15%, respectively. The lowest calibration point achieving accuracy within ±20% of the nominal value and coefficient of variation (CV) <20% were considered as the LLOQs for the targeted analytes.

2.8. Implementation of Correction Factors for Analysis of Different Plasma Types Through BHM

Calibration curves (area response of analyte/ISD response ratio vs analyte concentration) for the plasma samples from the four species (human, rat, rabbit, bovine) and PBS were fit jointly using a BHM according to the equation below:[16,17]

$$\log(y_{ij}) = \beta_{0j} + \beta_{1j}\log(x_{ij}) + \epsilon_{ij}$$
$$\begin{pmatrix}\beta_{0j}\\ \beta_{1j}\end{pmatrix} \sim N\left(\begin{pmatrix}\mu_0\\ \mu_1\end{pmatrix}, \Sigma\right) \quad (1)$$

where index ij represents the i^{th} observation from the j^{th} medium, μ_0 and μ_1 are the overall mean of the regression coefficients β_0 and β_1, and Σ is the variance−covariance matrix. The hierarchical model estimates medium-specific calibration curves (represented by β_{0j} and β_{1j}) and links all calibration curves by the hyperdistribution $N\left(\begin{pmatrix}\mu_0\\ \mu_1\end{pmatrix}, \Sigma\right)$. We can view the hyperdistribution as the common prior distribution of the five sets of calibration curve parameters, reflecting our precalibration assumption about the five curves: the parameters of the five curves are different (hence indexed by j), but we do not know how they differ from each other (hence the parameters are random variables) and related (measuring the same chemical, hence the common prior). Using the traditional linear regression calibration curve, parameters (β_{0j}^{MLE} and β_{1j}^{MLE}) are estimated by fitting the curves separately. The hierarchical estimated parameters (i.e., β_{0j}^{H} and β_{1j}^{H}) are closer to the overall means μ_0 and μ_1, respectively, than are β_{0j}^{MLE} and β_{1j}^{MLE}. This is known as the hierarchical model's shrinkage effect. Intuitively, we know that estimated regression parameters are with error (i.e., they are either too high or too low). With only one estimate, we have no reference to judge whether the estimate is too high or too low. With estimates from multiple regression parameters, the overall mean provides a likely reference, and shrinking estimated parameters toward it can improve the estimation accuracy. The hierarchical model estimated regression parameters are less likely to have extremely large or small values. Estimated β_{0j}^{H} and β_{1j}^{H} were applied to define a medium-specific calibration curve.

3. RESULTS AND DISCUSSION

3.1. SPME Method Optimization

Pesticides and pharmaceuticals used for this study showed acceptable retention in a C_{18} chromatographic column, which also indicates affinity of analytes toward SPME C18 extraction phase.[18] Therefore, the C18/PAN extraction phase was selected for SPME analysis. Considering the diverse physical and chemical properties of the targeted analytes, the desorption and extraction conditions of the method were optimized. Desorption parameters were optimized by tuning the solvent composition and time necessary for desorption. It has been demonstrated in the literature that ACN has the ability to desorb nonpolar pesticides and pharmaceuticals from the extraction phase, while a combination of MeOH and ACN has the ability to desorb polar pesticides and pharmaceuticals.[19] Furthermore, formic acid was included in the desorption solution to enhance the stability of the analyte.[19] Therefore, several combinations of MeOH, ACN, and water with 0.1% formic acid were evaluated as desorption solutions to achieve maximum desorption and minimum analyte

https://doi.org/10.1021/acsmeasuresciau.3c00049
ACS Meas. Sci. Au 2024, 4, 127−135

carryover in the fiber (Figure S1). The following solvent mixtures containing water and 0.1% formic acid were tested for desorption optimization: ACN:water (1:1, v:v) with 0.1% formic acid, MeOH:water (1:1, v:v) with 0.1% formic acid, ACN:MeOH:water (2:2:1, v:v:v) with 0.1% formic acid, ACN:MeOH:water (1:3:1, v:v:v) with 0.1% formic acid. The fiber desorption was conducted for 90 min with 320 μL of desorption solution in glass vials containing inserts. Followed by the first desorption, a second desorption was conducted in fresh aliquots of respective desorption solutions to assess analytes' carryover in each desorption solution (Figure S2).

According to the results obtained (Figure S1), the desorption solution of ACN:MeOH:H_2O (2:2:1, v:v:v) + 0.1% FA showed higher overall desorption of pharmaceuticals and comparable desorption of pesticides compared to the desorption solution of ACN:MeOH:H_2O (1:3:1, v:v:v) + 0.1% FA. Moreover, fiber carryover of analytes desorbed in ACN:MeOH:H_2O (2:2:1, v:v:v) + 0.1% FA solution remained <1%. However, as evident in Figure S1, the response for omeprazole was significantly lower compared to other analytes. Literature reports that although the addition of formic acid in desorption solution helps to increase the stability of the analytes, it can also cause conversion of the omeprazole in sulfenic acid or cyclic sulfonamides.[20] Therefore, to evaluate the effect of formic acid on omeprazole, an ACN:MeOH:water (2:2:1, v:v:v) desorption solution was tested with and without formic acid (Figure S3). The response for omeprazole in the desorption solution without formic acid increased by 99.5% compared with the desorption solution with formic acid. Therefore, the desorption solution of MeOH:ACN:water (2:2:1, v:v:v) without formic acid was used for further studies.

Once the optimum desorption solution was selected, a desorption time profile was conducted from 10 to 90 min to find out the minimum desorption time that can use to desorb analytes with <1% analytes carryover in the SPME fiber (Figure S4). To determine the carryover percentage at each time interval in the desorption time profile, the second desorption was conducted 90 min after the first desorption of the fiber (Figure S5). Figure S4 shows the amounts of analytes desorbed over different time intervals. The amount of analyte desorbed did not significantly change over the tested time. By compromise of both analyte throughput and the carryover value, the optimal desorption time for the further experiment was selected as 20 min.

Under the optimized desorption conditions, an extraction time profile was conducted to select the optimum conditions for fiber extraction. Extraction time profiles were acquired from 10 to 90 min in both pooled bovine plasma and PBS. PBS was selected to simulate plasma pH and salinity; however, PBS does not contain macromolecules, such as proteins, that can bind with the analytes and cause matrix effects on the analysis. Therefore, PBS can serve as a reference to study the matrix effects and analyte−PPB in the blood plasma. The results in Figure 1 show that the equilibrium was achieved for analytes extractions in both bovine plasma and PBS at 45 min. Therefore, 45 min was selected as the fiber extraction time for the method validation and matrix effect evaluation studies. In Table S5, the absolute recovery percentages of analytes during the extraction from PBS and bovine plasma were shown at each time point. Analytes present in bovine plasma have a lower free concentration than analytes present in PBS due to analyte PPB. In SPME, the amount of analyte extracted is proportional to the initial free concentration of the analyte. As a result, the absolute recovery % values for extractions from PBS were higher than those obtained in bovine plasma. In this regard, it appears that different analytes bind to plasma protein to different extents, which can cause binding related-matrix effects for microextraction.

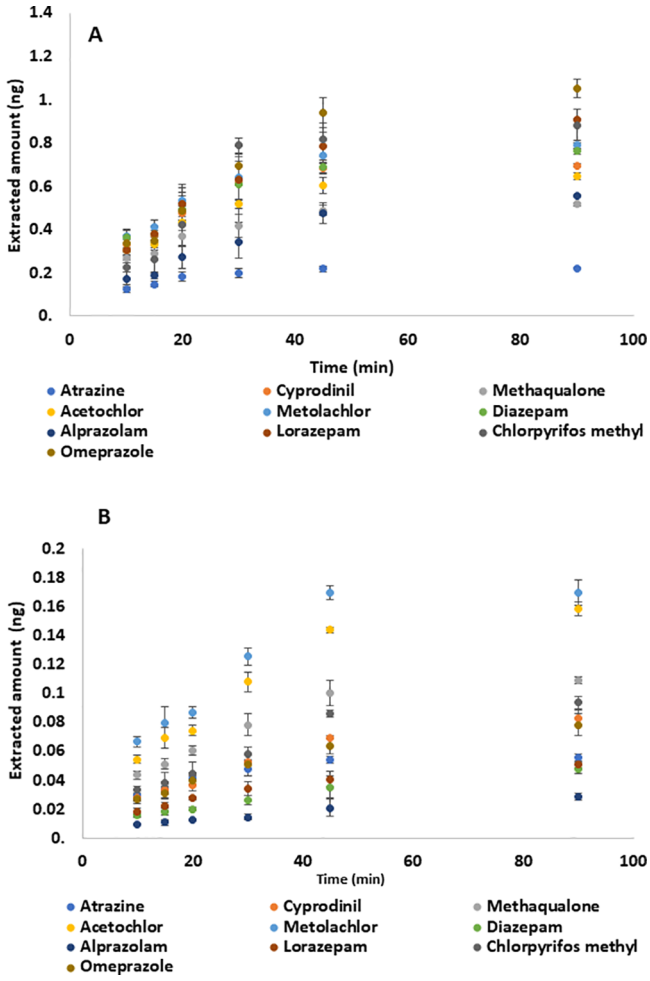

Figure 1. Extraction time profile acquired in (A) PBS and (B) bovine plasma. The desorption was conducted using 320 μL of MeOH:ACN:water (2:2:1, v:v:v) solution was left for 20 min.

3.2. Matrix Effect Evaluation

In LC−MS, matrix effects occur when coeluting species change the relative efficiency of the ionization process by either enhancing or inhibiting charge transfer to the target analyte and forming ions in the gas phase. In particular, matrix effects are dependent on the type of plasma analyzed; matrix components of different plasma types may cause ion suppression or enhancement effects to varying degrees. Therefore, it is essential to evaluatematrix effects for each plasma type according to the US FDA guidelines on bioanalytical analysis to identify bias among measurements in interspecies plasma . According to the FDA guidelines, matrix effects should not be present during biological samples analysis.[21] The accuracy of the measurement should be ±15% of the nominal concentration for each matrix evaluated, and the precision of the measurement should not exceed 15%.[8,10,11]

The quantitative evaluation of the matrix effects was carried out according to the method proposed by Matuszewski et al.[22] The absolute matrix effect was evaluated by spiking the plasma

https://doi.org/10.1021/acsmeasuresciau.3c00049
ACS Meas. Sci. Au 2024, 4, 127−135

Table 1. Absolute Matrix Effects for Targeted Analytes in Different Plasma Types (Bovine, Rat, Rabbit, Human)

matrix effect %	atrazine	cyprodinil	methaqualone	acetochlor	metolachlor	diazepam	alprazolam	chlorpyrifos methyl	lorazepam	omeprazole
bovine plasma	95.8	96.2	99.0	96.2	96.7	98.1	96.7	105.9	99.4	96.2
human plasma	103.4	103.8	102.1	104.6	104.7	102.0	98.9	106.1	99.9	96.4
rabbit plasma	101.9	105.5	106.5	100.7	102.3	105.1	104.9	106.0	108.3	105.9
rat plasma	103.2	107.9	119.0	104.3	106.4	109.9	107.5	160.3	98.8	109.3

from different species of mammals (e.g., bovine, rabbit, rat, and human) with a mixture of pesticide and drugs standards. In order to calculate the absolute matrix effects, the peak area of analytes spiked at a fixed concentration in a desorption solution obtained from SPME extractions of blank plasms ($A2$) was divided by the peak areas obtained from a spike in neat solvent (desorption solvent mixture) ($A1$).[21]

$$\text{Matrix effects\%} = \frac{\text{Area } (A2)}{\text{Area } (A1)} \times 100 \quad (2)$$

The absolute matrix effects % mentioned in Table 1 for all of the targeted analytes and plasma types were calculated using eq 2. As indicated in Table 1, the matrix effect values for all analytes in all types of plasma were approximately 100 ± 10% except for chlorpyrifos-methyl which had a matrix effect value of 160.3% in rat plasma. A higher matrix effect value for chlorpyrifos methyl in rat plasma could have occurred due to the coelution of specific matrix components in rat plasma with the analyte, enhancing the instrument response. According to overall results for the matrix effects, minimum or no matrix effect was recorded for the analysis of plasma from four different mammals. This indicates that the optimized SPME technique with a matrix-compatible SPME extraction phase (C_{18}/PAN) can minimize the instrumental absolute matrix effects for bioanalysis by preventing the coextraction of matrix components such as phospholipids, cholesterol, and glycerides. This finding allows to deconvolute causes of response variation for the targeted analytes within interspecies plasma, excluding interferences caused by absolute matrix effect (e.g., alteration of the ionization process of target analytes) and identify the effect of PPB on the extraction recoveries.

3.3. Assessment of the Potential for Cross-Matrix Calibration

To verify the quantitative performance of the optimized method, matrix-matched calibration curves were built for each of the mammalian plasma targeted in this study. The calibration range for all the analytes spanned in a concentration range between 0.01 and 100 $\mu g\ L^{-1}$. Table S6 shows the figures of merit for all of the analytes in each plasma type. Table S7 shows the measurements for accuracy at several concentration levels for QC samples calculated by using calibration curves in the respective plasma types. For all the analytes in different plasma, accuracy ranged from 80 to 120%, and precision was below 15%, indicating the suitability of this approach for high-accuracy measurements. Even though the optimized SPME method does not show matrix effects related to coeluting matrix interference during instrumental analysis, calibration curves from different plasma types displayed different slopes and intercepts, related to the varied composition of the mammalian plasma targeted and the extraction mechanism of SPME.

This study proposes a strategy to reduce the need for several measurements and calibration curves involving plasma samples not readily available and expensive to purchase such as human plasma. To verify the suitability of a cross-matrix calibration approach, QC samples prepared in human plasma were quantified but calculated using calibration curves prepared from other plasma types (bovine, rat, rabbit) and PBS (Table S8). This test indicates that most of the analytes tested display unacceptable accuracy, with values outside the acceptable range of 80−120%. Only diazepam and metolachlor showed acceptable values of accuracy for QC samples prepared in human plasma when quantified using cross-matrix calibration in PBS, rat, rabbit, and bovine plasma. Considering this phenomenon, further inspection of the calibration curves obtained in the different media tested revealed that slopes and intercepts of the calibration curves varied and depended on the physical−chemical properties of the analytes and the affinity of analytes for the plasma proteins in each plasma type.

3.4. Use of a BHM To Assess Correction Factors for Accurate Cross-Matrix Calibration

Differences in interspecies PPB for the targeted analytes resulted in calibration curves with different slopes and intercept values. Figure S6 shows the statistical differences in slope and intercepts of calibration curves conducted in different plasma types and PBS samples. The different slope and intercept values obtained did not provide satisfactory accuracy when cross-matrix calibration was used for quantification (Table S8). To ensure accurate measurements for method validation and sample quantification, matrix-matched calibration curves must be conducted separately for each type of plasma (as demonstrated in Table S7). In addition to being time-consuming, this process can also be expensive. To reduce the need for several measurements and matrix-matched calibration curves, we used a BHM approach to obtain correction factors to allow cross-matrix calibration. For this reason, calibration curves for the plasma samples from four species and PBS were fitted using a BHM approach as described in Section 2.8. Mathematical studies have consistently shown that the BHM approach outperforms traditional estimation methods that would fit calibrants separately.[23]

Qian et al. summarized the practical benefit of using the BHM approach and illustrated how the BHM approach improved estimation accuracy in measuring cyanobacterial toxins concentration in drinking water.[24,25] Also, the use of hierarchical modeling for reducing measurement uncertainty in calibration-curve methods was broadly discussed in the literature.[25] For this study, exploratory data plots were used to show that the calibration curve should be a log−log linear regression model (Figures S7). The log−log linear relationship between the response and the analyte concentration reflects our understanding of the process (that a fixed proportional response is expected for a fixed increase in the concentration). In this study, a 1% increase in response was observed for every 1% increase in concentration (Figure S7). That is, the measured response (area response, y) is proportional to the analyte concentration (x). In other words, in the original scale, the curve can be expressed as $y = ax$. In the logarithmic scale,

https://doi.org/10.1021/acsmeasuresciau.3c00049
ACS Meas. Sci. Au 2024, 4, 127−135

Table 2. Calculated Correction Factors for the Calibration Curves in Bovine, Human, PBS, Rabbit, and Rat Plasma

analytes	media	β_0 = mean intercept	β_1 = mean slope	C_0 = intercept correction factor	C_1 = slope correction factor
metolachlor	bovine plasma	2.37	0.99	0.194	0.016
	human plasma	2.18	0.98	0.000	0.000
	PBS	2.37	0.98	0.191	0.004
	rabbit plasma	2.20	0.98	0.021	0.003
	rat plasma	2.25	0.99	0.078	0.014
alprazolam	bovine plasma	0.37	1.00	−0.337	0.058
	human plasma	0.70	0.94	0.000	0.000
	PBS	0.45	0.95	−0.253	0.004
	rabbit plasma	−1.52	0.99	−2.227	0.047
	rat plasma	−0.15	1.03	−0.854	0.092
diazepam	bovine plasma	0.81	0.98	−0.041	0.081
	human plasma	0.85	0.90	0.000	0.000
	PBS	0.80	0.99	−0.047	0.087
	rabbit plasma	0.82	0.99	−0.025	0.087
	rat plasma	0.81	0.99	−0.033	0.088
cyprodinil	bovine plasma	−1.37	1.00	1.846	0.072
	human plasma	−3.22	0.93	0.000	0.000
	PBS	3.95	1.04	7.172	0.116
	rabbit plasma	−2.72	0.98	0.503	0.058
	rat plasma	−2.76	0.98	0.460	0.057
chlorpyrifos methyl	bovine plasma	−1.61	0.98	0.586	0.036
	human plasma	−2.19	0.94	0.000	0.000
	PBS	−1.64	1.00	0.555	0.057
	rabbit plasma	−2.18	1.03	0.010	0.089
	rat plasma	−2.25	0.97	−0.062	0.029
acetochlor	bovine plasma	−0.30	1.03	0.502	−0.051
	human plasma	−0.80	1.08	0.000	0.000
	PBS	−0.33	1.00	0.476	−0.082
	rabbit plasma	−0.77	1.12	0.033	0.041
	rat plasma	−0.85	1.02	−0.045	−0.066
lorazepam	bovine plasma	0.77	1.00	−0.897	0.048
	human plasma	1.67	0.95	0.000	0.000
	PBS	1.13	0.99	−0.536	0.033
	rabbit plasma	0.66	0.94	−1.003	−0.012
	rat plasma	0.70	0.98	−0.963	0.028
omeprazole	bovine plasma	−1.25	0.77	−0.007	0.079
	human plasma	−1.24	0.69	0.000	0.000
	PBS	−1.05	0.78	0.188	0.094
	rabbit plasma	−0.92	0.97	0.323	0.280
	rat plasma	−1.24	1.01	−0.004	0.324
atrazine	bovine plasma	−0.94	1.01	3.344	0.135
	human plasma	−4.29	0.87	0.000	0.000
	PBS	−0.70	0.89	3.581	0.016
	rabbit plasma	−3.99	1.02	0.294	0.146
	rat plasma	−3.00	1.10	1.285	0.226
methaqualone	bovine plasma	1.74	1.02	1.809	0.035
	human plasma	−0.07	0.98	0.000	0.000
	PBS	0.36	0.90	0.428	−0.082
	rabbit plasma	−3.05	1.03	−2.980	0.044
	rat plasma	−1.69	1.06	−1.627	0.079

the curve is "log"(y) = "log"(a) + "log"(x) or more generally "log"(y) = β_0 + β_1 "log"(x) + ϵ. A log−log scale provides an additional measure of experimental quality by estimating the calibration curve slope β_1. The slope (β_1) should be only slightly less than 1 (because of the regression to the mean effect), and the matrix effect can be estimated in the differences in the intercepts among the five different media. To further enhance the estimation accuracy of the calibration curve coefficients (β_0 and β_1), the calibration data from the five media were combined to form a BHM which is described in Section 2.8. The β_0 (mean intercept) and β_1 (mean slope) were calculated for the generated calibration curves for each medium using BHM. Then, the intercept correction factor (C_0) and the slope correction factor (C_1) were calculated considering human plasma calibration curve values (β_0 and β_1) as a reference. Therefore, the C_0 and C_1 values for analytes in human plasma were calculated as zero.

The intercept correction factor (C_0) was calculated for four different plasma types and PBS by using eq 3:

$$C_0 = \beta_{0_{\text{humanplasmacalcurve}}} - \beta_0 x \tag{3}$$

where $\beta_0 x$ is the β_0 value obtained from the human, bovine, rat, rabbit plasma, and PBS. The slope correction factor (C_1) was calculated for four different plasma types and PBS using eq 4

$$C_1 = \beta_{1_{\text{humanplasmacalcurve}}} - \beta_1 x \tag{4}$$

The calculated C_0 and C_1 values for each analyte extracted from human, rat, rabbit, bovine plasma, and PBS are listed in Table 2.

The following equations were used to calculate the concentration and accuracy obtained for QC samples prepared

https://doi.org/10.1021/acsmeasuresciau.3c00049
ACS Meas. Sci. Au 2024, 4, 127−135

Table 3. Calculated Accuracy for the Concentrations Obtained for QC Samples of Human Plasma Using Corrected Calibration Curves from Bovine, Rat, Rabbit Plasma, and PBS[a]

analytes	human plasma QC sample concentration ($\mu g\ L^{-1}$)	accuracy % obtained by matrix-matched calibration in human plasma	accuracy % obtained by cross-matrix calibration calculated using eq 5				accuracy % obtained by cross-matrix calibration calculated using eq 6				accuracy % obtained by cross-matrix calibration calculated using eq 7				accuracy % obtained by cross-matrix calibration calculated using eq 8			
			media				media				media				media			
			bovine	PBS	rabbit	rat	bovine	PBS	rabbit	rat	bovine	PBS	rabbit	rat	bovine	PBS	rabbit	rat
metolachlor	2.5	104.8	98.9	98.9	98.9	98.9	104.0	100.1	99.8	103.2	81.1	81.4	96.8	91.4	85.5	82.4	97.7	95.4
	25.0	105.0	102.7	102.7	102.7	102.7	103.9	103.0	102.9	103.7	84.2	84.5	100.6	94.9	85.4	84.8	100.8	95.9
	75.0	111.7	110.3	112.1	112.1	112.1	111.1	111.9	111.9	111.3	91.9	92.2	109.7	103.5	91.4	92.1	109.6	102.9
alprazolam	2.5	96.6	91.7	91.7	91.7	91.7	109.8	93.0	106.2	120.6	131.3	120.0	976.4	227.3	153.9	121.6	1010.2	275.6
	25.0	98.7	97.4	97.4	97.4	97.4	101.6	97.7	100.8	103.8	139.3	127.4	1036.6	241.3	142.3	127.7	958.8	237.3
	75.0	93.8	98.0	98.0	98.0	98.0	95.8	97.8	96.2	94.7	140.2	128.2	1042.6	242.7	134.2	127.8	915.1	216.5
diazepam	2.5	104.8	97.1	96.6	97.1	97.1	124.8	126.9	126.9	127.2	101.1	101.8	99.3	100.2	129.5	132.4	129.5	130.8
	25.0	105.0	89.5	89.0	89.5	89.5	95.7	96.1	96.1	96.2	93.2	93.8	91.5	92.4	99.2	100.3	98.1	98.9
	75.0	111.7	96.2	95.8	96.2	96.2	93.4	93.2	93.2	93.2	100.2	100.9	98.4	99.3	96.9	97.2	95.1	95.9
cyprodinil	2.5	95.2	90.3	90.3	90.3	90.3	112.8	127.7	108.4	108.1	12.3	0.04	52.4	55.0	17.7	0.1	65.0	67.7
	25.0	94.1	92.3	92.3	92.3	92.3	97.5	100.6	96.6	96.5	12.5	0.04	53.6	56.1	15.3	0.1	57.9	60.4
	75.0	94.0	99.5	99.5	99.5	99.5	96.6	95.1	97.1	97.2	13.5	0.04	57.7	60.5	15.2	0.1	58.2	60.8
chlorpyrifos methyl	2.5	100.0	96.1	96.1	96.1	96.1	107.7	114.4	125.0	105.1	51.6	53.3	95.1	102.7	59.1	65.5	123.8	112.1
	25.0	93.2	91.4	91.4	91.4	91.4	94.1	95.6	97.8	93.5	49.0	50.6	90.4	97.6	51.6	54.8	96.9	99.7
	75.0	95.5	99.5	99.5	99.5	99.5	98.1	97.3	96.1	98.4	53.4	55.2	98.5	106.3	53.8	55.8	95.2	104.9
acetochlor	2.5	94.8	102.0	102.0	102.0	102.0	88.1	79.8	113.6	84.2	64.2	65.7	99.0	106.4	54.2	49.6	110.4	87.9
	25.0	95.7	101.2	101.2	101.2	101.2	97.8	95.7	103.7	96.8	63.6	65.2	98.2	105.5	60.1	59.4	100.7	101.2
	75.0	104.6	102.3	102.3	102.3	102.3	104.4	105.9	100.7	105.1	64.3	65.9	99.2	106.6	64.2	65.8	97.8	109.9
lorazepam	2.5	106.9	101.2	101.2	101.2	101.2	116.9	111.7	97.3	110.1	259.0	177.4	289.5	277.6	285.9	192.2	282.2	293.5
	25.0	104.7	106.5	106.5	106.5	106.5	109.8	108.8	105.7	108.5	272.8	186.8	304.8	292.3	268.7	187.2	306.5	289.2
	75.0	98.6	105.1	105.1	105.1	105.1	102.8	103.5	105.8	103.8	269.1	184.3	300.8	288.4	251.6	178.2	306.8	276.8
omeprazole	5.0	106.9	77.4	77.4	58.0	58.0	100.7	105.2	121.8	131.9	78.2	58.9	36.3	58.4	101.7	82.7	116.3	176.6
	50.0	94.2	100.5	100.5	75.4	75.4	100.5	100.5	75.3	75.3	101.6	76.5	47.1	75.9	101.5	79.0	71.9	100.8
atrazine	5.0	108.1	111.2	111.2	111.2	111.2	149.5	115.6	152.5	174.8	2.4	1.8	79.3	25.4	5.4	2.0	114.1	54.1
	50.0	106.6	117.2	117.2	117.2	117.2	114.7	116.9	114.6	113.4	2.5	1.9	83.6	26.8	4.1	2.0	85.7	35.1
methaqualone	2.5	91.9	91.0	91.0	91.0	91.0	101.3	68.6	104.0	114.6	14.5	58.9	1882.0	475.7	17.2	42.7	1886.9	529.5
	25.0	94.6	97.2	97.2	97.2	97.2	99.6	91.0	100.2	102.6	15.4	62.9	2009.7	508.0	16.9	56.6	1819.5	473.9
	75.0	100.9	105.5	105.5	105.5	105.5	103.9	110.1	103.5	102.0	16.8	63.3	2182.8	551.8	17.6	68.5	1878.2	471.3

[a]Highlighted values in the table indicate unacceptable accuracy, which falls outside the 80−120% range.

https://doi.org/10.1021/acsmeasuresciau.3c00049
ACS Meas. Sci. Au 2024, 4, 127−135

in human plasma using calibration curves conducted in rat, rabbit, bovine plasma, and PBS.

$$\text{Calculated concentration of the QC sample} = \exp\left(\ln(50) + \left(\frac{\ln\left(\frac{\text{peak area}}{\text{ISD ratio}}\text{ for QC sample}\right) - (\beta_0 - C_0)}{\beta_1 - C_1}\right)\right) \quad (5)$$

$$\text{Calculated concentration of the QC sample} = \exp\left(\ln(50) + \left(\left(\ln\left(\frac{\text{peak area}}{\text{ISD ratio}}\text{ for QC sample}\right) - (\beta_0 - C_0)\right)/(\beta_1)\right)\right) \quad (6)$$

$$\text{Calculated concentration of the QC sample} = \exp\left(\ln(50) + \left(\left(\ln\left(\frac{\text{peak area}}{\text{ISD ratio}}\text{ for QC sample}\right) - (\beta_0)\right)/(\beta_1 - C_1)\right)\right) \quad (7)$$

$$\text{Calculated concentration of the QC sample} = \exp\left(\ln(50) + \left(\left(\ln\left(\frac{\text{peak area}}{\text{ISD ratio}}\text{ for QC sample}\right) - (\beta_0)\right)/(\beta_1)\right)\right) \quad (8)$$

By the use of eq 5, both intercept correction and slope correction factors were applied to quantify the tested QC samples. eqs 6 and 7 were applied using the intercept correction factor (C_0) and slope correction factor (C_1), respectively, to determine the concentration of the QC samples. Correction factors are not included in eq 8. Tables 3 and S9 show the calculated accuracy and concentration for each QC sample in human plasma using eqs 5−8 and provide, as reference values, the accuracy and concentration calculated using matrix-matched calibration obtained in human plasma. Accuracy values calculated using corrected concentration (by using both C_1 and C_0 eq 5) showed acceptable values, within the 80−120% range. According to eq 6 (which only contains intercept correction factor C_0) and eq 7 (which only contains slope correction factor C_1), a higher degree of accuracy can be achieved using only the intercept correction factor. In fact, the slope correction factor C_1 did not yield an acceptable accuracy for most of the analytes tested. This suggests that the intercept of the calibration curves derived from different media has an effect on quantification, which could be related to the different extent of PPB levels of the analytes. The accuracy values calculated using eq 8 which did not contain any correction factors, were either higher than or below acceptable limits, indicating that correction factors are essential tocorrect measurements obtained using calibration curves conducted in other plasma types other than human plasma. The process flowchart for applying BHM to obtain correction factors for accurate cross-matrix calibration is shown in Figure S8.

4. CONCLUSIONS

This work demonstrates a convenient and robust workflow for the assessment of xenobiotics in interspecies plasma via bio-SPME-LC-MS. The developed method simultaneously extracted xenobiotics from different mammalian species' blood plasma with minimized instrumental matrix effects,that ranged from 96.2 to 109.3%. These findings indicate that the biocompatible C18/PAN extraction phase was able to reduce matrix effects caused by coeluting macromolecules. The developed SPME method displayed LOQs in the range of 0.01−1 $\mu g\ L^{-1}$ and a linear dynamic range of 0.01−100 $\mu g\ L^{-1}$. Although the occurrence of instrumental matrix effects was minimized, as attested by the figures of merit obtained via matrix-matched calibration; quantification of human plasma samples via cross-matrix calibration did not reveal satisfactory performance. To address this, a combined approach of cross-matrix calibration and BHM was employed to determine correction factors, effectively mitigating measurement bias within interspecies blood plasma. For all analytes extracted from human plasma, the slope correction factor (C_1) and intercept correction factor (C_0) were used to achieve accuracy levels within 80−120% using cross-matrix calibration . The results demonstrate that employing both correction factors, C_1 and C_0, enables accurate cross-matrix calibration for quantifying xenobiotics in human plasma samples, even when calibration curves are prepared in different media. The intercept correction factor (C_0) was found to be more influential in correction performance compared to the slope correction factor (C_1). The developed methodology and statistical model successfully mitigate the bias of interplasma species measurements, representing a convenient and alternative strategy to minimize the consumption of mammalian plasma difficult to access. This work also establishes a new strategy for high-accuracy measurements applicable to biomonitoring and pharmacokinetic studies.

■ ASSOCIATED CONTENT

Supporting Information

The Supporting Information is available free of charge at https://pubs.acs.org/doi/10.1021/acsmeasuresciau.3c00049.

Model analytes physicochemical properties, LC-MS/MS operational parameters, results of method development, figures of merit of the validated method, results of BHM computation (PDF)

■ AUTHOR INFORMATION

Corresponding Author

Emanuela Gionfriddo − *Department of Chemistry and Biochemistry, College of Natural Sciences and Mathematics, School of Green Chemistry and Engineering, and Dr. Nina McClelland Laboratory for Water Chemistry and Environmental Analysis, The University of Toledo, Toledo, Ohio 43606, United States;* orcid.org/0000-0002-1836-1950; Email: emanuela.gionfriddo@utoledo.edu

https://doi.org/10.1021/acsmeasuresciau.3c00049
ACS Meas. Sci. Au 2024, 4, 127−135

Authors

Nipunika H. Godage − *Department of Chemistry and Biochemistry, College of Natural Sciences and Mathematics, School of Green Chemistry and Engineering, and Dr. Nina McClelland Laboratory for Water Chemistry and Environmental Analysis, The University of Toledo, Toledo, Ohio 43606, United States*

Song S. Qian − *Department of Environmental Sciences, The University of Toledo, Toledo, Ohio 43606, United States;* orcid.org/0000-0002-2346-4903

Erasmus Cudjoe − *PerkinElmer Inc., Woodbridge, Ontario L4L 8H1, Canada*

Complete contact information is available at: https://pubs.acs.org/10.1021/acsmeasuresciau.3c00049

Author Contributions

CRediT: **Nipunika H Godage** data curation, formal analysis, investigation, methodology, validation, writing-original draft; **Song S. Qian** data curation, funding acquisition, investigation, methodology, software, visualization; **Erasmus Cudjoe** methodology, resources, validation; **Emanuela Gionfriddo** conceptualization, data curation, funding acquisition, project administration, supervision, writing-review & editing.

Notes

The authors declare no competing financial interest.

■ ACKNOWLEDGMENTS

The authors would like to acknowledge the University of Toledo for funding. Also, authors would like to express their gratitude to Millipore Sigma for providing the SPME devices used in this study.

■ REFERENCES

(1) Needham, L. L.; Calafat, A. M.; Barr, D. B. Uses and Issues of Biomonitoring. *Int. J. Hyg. Environ. Health* **2007**, *210* (3−4), 229−238.

(2) Alves, A.; Kucharska, A.; Erratico, C.; Xu, F.; Den Hond, E.; Koppen, G.; Vanermen, G.; Covaci, A.; Voorspoels, S. Human Biomonitoring of Emerging Pollutants through Non-Invasive Matrices: State of the Art and Future Potential. *Anal. Bioanal. Chem.* **2014**, *406* (17), 4063−4088.

(3) Panuwet, P.; Hunter, R. E. H., Jr; D'Souza, P. E.; Chen, X.; Radford, A.; Cohen, J. R.; Marder, M. E.; Kartavenka, K.; Ryan, P. B.; Barr, D. B. Biological Matrix Effects in Quantitative Tandem Mass Spectrometry-Based Analytical Methods: Advancing Biomonitoring. *Crit. Rev. Anal. Chem.* **2016**, *46* (2), 93−105.

(4) Zhou, W.; Yang, S.; Wang, P. G. Matrix Effects and Application of Matrix Effect Factor. *Bioanalysis* **2017**, *9* (23), 1839−1844.

(5) Barr, D. B.; Wilder, L. C.; Caudill, S. P.; Gonzalez, A. J.; Needham, L. L.; Pirkle, J. L. Urinary Creatinine Concentrations in the U.S. Population: Implications for Urinary Biologic Monitoring Measurements. *Environ. Health Perspect.* **2005**, *113* (2), 192−200.

(6) Guo, X.; Lankmayr, E. Phospholipid-Based Matrix Effects in LC-MS Bioanalysis. *Bioanalysis* **2011**, *3* (4), 349−352.

(7) Godage, N. H.; Gionfriddo, E. Biocompatible SPME Coupled to GC/MS for Analysis of Xenobiotics in Blood Plasma. *J. Chromatogr., B: Anal. Technol. Biomed. Life Sci.* **2022**, *1203*, No. 123308.

(8) Gray, N. P.; McDougall, S. A.; Dean, J. R. Analytical Bias between Species Caused by Matrix Effects in Quantitative Analysis of a Small-Molecule Pharmaceutical Candidate in Plasma. *Bioanalysis* **2012**, *4* (6), 675−684.

(9) Colclough, N.; Ruston, L.; Wood, J. M.; MacFaul, P. A. Species Differences in Drug Plasma Protein Binding. *Medchemcomm* **2014**, *5* (7), 963−967.

(10) Rogatsky, E.; Stein, D.; Toxicology, F.; Workplace, F.; Testing, D.; Toxicology, P. F.; Fachi, M. M.; Leonart, L. P.; Cerqueira, L. B.; Pontes, F. L. D.; et al. Bioanalytical Method Validation Guidance. *J. Chromatogr. B Anal. Technol. Biomed. Life Sci.* **2017**, *1043*, 25.

(11) Smith, G. Bioanalytical Method Validation: Notable Points in the 2009 Draft EMA Guideline and Differences with the 2001 FDA Guidance. *Bioanalysis* **2010**, *2* (5), 929−935.

(12) Jemal, M.; Huang, M.; Jiang, X.; Mao, Y.; Powell, M. L. Direct Injection versus Liquid-Liquid Extraction for Plasma Sample Analysis by High Performance Liquid Chromatography with Tandem Mass Spectrometry. *Rapid Commun. Mass Spectrom.* **1999**, *13* (21), 2125−2132.

(13) Vuckovic, D.; Zhang, X.; Cudjoe, E.; Pawliszyn, J. Solid-Phase Microextraction in Bioanalysis: New Devices and Directions. *J. Chromatogr. A* **2010**, *1217* (25), 4041−4060.

(14) Polson, C.; Sarkar, P.; Incledon, B.; Raguvaran, V.; Grant, R. Optimization of Protein Precipitation Based upon Effectiveness of Protein Removal and Ionization Effect in Liquid Chromatography-Tandem Mass Spectrometry. *J. Chromatogr. B Anal. Technol. Biomed. Life Sci.* **2003**, *785* (2), 263−275.

(15) Gionfriddo, E. Recent Developments in LC Column Technology. *Suppl. LCGC North Am.* **2020**, *38* (s6), 25−28.

(16) Qian, S. S.; Stow, C. A.; Nojavan, A. F.; Stachelek, J.; Cha, Y.; Alameddine, I.; Soranno, P. The Implications of Simpson's Paradox for Cross-Scale Inference among Lakes. *Water Res.* **2019**, *163*, No. 114855.

(17) Qian, P. Z. G.; Wu, C. F. J. Bayesian Hierarchical Modeling for Integrating Low-Accuracy and High-Accuracy Experiments. *Technometrics* **2008**, *50* (2), 192−204.

(18) Roy, K. S.; Nazdrajić, E.; Shimelis, O. I.; Ross, M. J.; Chen, Y.; Cramer, H.; Pawliszyn, J. Optimizing a High-Throughput Solid-Phase Microextraction System to Determine the Plasma Protein Binding of Drugs in Human Plasma. *Anal. Chem.* **2021**, *93* (32), 11061−11065.

(19) Geerdink, R. B.; Kooistra-Sijpersma, A.; Tiesnitsch, J.; Kienhuis, P. G. M.; Brinkman, U. A. T. Determination of Polar Pesticides with Atmospheric Pressure Chemical Ionisation Mass Spectrometry-Mass Spectrometry Using Methanol and/or Acetonitrile for Solid-Phase Desorption and Gradient Liquid Chromatography. *J. Chromatogr. A* **1999**, *863* (2), 147−155.

(20) DellaGreca, M.; Iesce, M. R.; Previtera, L.; Rubino, M.; Temussi, F.; Brigante, M. Degradation of Lansoprazole and Omeprazole in the Aquatic Environment. *Chemosphere* **2006**, *63* (7), 1087−1093.

(21) Birjandi, A. P.; Mirnaghi, F. S.; Bojko, B.; Wąsowicz, M.; Pawliszyn, J. Application of Solid Phase Microextraction for Quantitation of Polyunsaturated Fatty Acids in Biological Fluids. *Anal. Chem.* **2014**, *86* (24), 12022−12029.

(22) Matuszewski, B. K.; Constanzer, M. L.; Chavez-Eng, C. M. Matrix Effect in Quantitative LC/MS/MS Analyses of Biological Fluids: A Method for Determination of Finasteride in Human Plasma at Picogram Per Milliliter Concentrations. *Anal. Chem.* **1998**, *70* (5), 882−889.

(23) Efron, B. The Future of Indirect Evidence. *Stat. Sci.* **2010**, *25* (2), 145−157.

(24) Qian, S. S.; Stow, C. A.; Cha, Y. Implications of Steins Paradox for Environmental Standard Compliance Assessment. *Environ. Sci. Technol.* **2015**, *49* (10), 5913−5920.

(25) Qian, S. S.; Chaffin, J. D.; Dufour, M. R.; Sherman, J. J.; Golnick, P. C.; Collier, C. D.; Nummer, S. A.; Margida, M. G. Quantifying and Reducing Uncertainty in Estimated Microcystin Concentrations from the ELISA Method. *Environ. Sci. Technol.* **2015**, *49* (24), 14221−14229.